

Flux enhancement model for cold cesium fine-structure changing collisions

A. Fioretti^{1,a}, E. Arimondo^{1,b}, and A. Crubellier²¹ Istituto Nazionale per la Fisica della Materia, Dipartimento di Fisica, Università di Pisa, via Buonarroti 2, 56127 Pisa, Italy² Laboratoire Aimé Cotton^c, CNRS II, Bâtiment 505, Campus d'Orsay, 91405 Orsay Cedex, France

Received 22 July 1999 and Received in final form 4 May 2000

Abstract. The measurements of fine-structure changing collisions in a cesium magneto-optical trap, reported in a previous work [A. Fioretti *et al.*, Phys. Rev. A **55**, R3999 (1997)], are reanalyzed within a model based on the flux enhancement effect, which takes place in cold atomic collisions. In the present analysis, we consider the cooperative effect of the long-range and the shorter-range excitation by the strong trap laser. We evidence also the important role of the hyperfine structure of the Cs₂ molecular levels asymptotically connected to the 6S_{1/2} + 6S_{1/2} ground-state and 6S_{1/2} + 6P_{3/2} excited-state dissociation limits.

PACS. 34.50.Rk Laser-modified scattering and reactions – 32.80.Pj Optical cooling of atoms; trapping

1 Introduction

In these last ten years, the development of laser cooling techniques has provided experimentalists with samples of alkali, alkaline-earth, and metastable rare atoms in the microKelvin range and below. Among the several exciting studies permitted by the matter in this extreme condition, the subject of collisions between laser cooled atoms in presence of resonant laser fields has been the object of a broad experimental and theoretical interest [1–3]. Cold atoms undergoing inelastic collisions can receive enough energy to escape the atomic trap where they are confined. In particular, excited state collisions between one atom in its ground-state and one in its first-excited state are unavoidable in a magneto-optical trap (MOT), and contribute to limit the maximum density and total number of trapped atoms, and the reaching of very low temperatures.

Two leading inelastic mechanisms that affect singly-excited-state collisions are the so called “radiative escape” (RE), and “fine-structure change” (FSC). They are best described in a molecular environment [1–3]. Briefly, in RE the atomic pair, photoexcited by the quasisonant laser, spontaneously decays through the emission of a red-detuned photon. The energy difference between absorbed and emitted photons is shared by the two colliding partners as extra kinetic energy, which can be large enough to make both atoms escape the trap. Differently, in FSC, the colliding pair, excited by the laser on the D_2 line to the upper fine-structure state, survives radiatively until

short internuclear distance are reached. Here, a transition to the lower energy excited state takes place, again leaving the fine-structure energy difference as kinetic energy of the two atoms, which is generally large enough to produce trap loss. Finally, the excited atom decays emitting a photon on the D_1 line.

While several experiments measured the total loss rate from a MOT [1–3], the interplay between RE and FSC mechanisms has been tested in a few recent investigations. In reference [4] we measured for the first time the absolute trap loss rate coefficient for cesium FSC collisions, by directly detecting the fluorescence yield on the D_1 cesium line. Those measurements, performed as a function of trapping laser intensity and of hyperfine (HF) state occupation, were analyzed on the basis of atomic transfer, during optical collision, between HF ground states. Later, Wang *et al.* [5] used predissociation due to FSC to perform high resolution photoassociation spectroscopy of the attractive molecular excited states in potassium. No attempt has however been made in this experiment to derive the FSC trap loss rate coefficient. Very recently, precise new measurements for FSC trap loss rate coefficients have been obtained. In reference [6], the detection of the emitted D_1 photons allowed the measurement of the ratio of the FSC to the RE rate coefficient in cesium as a function of the trapping laser intensity. In reference [7], ionization of the atoms experiencing FSC allowed a direct measurement of the FSC rate in rubidium.

In a different context, recent experiments [8–14] of cold optical collisions in alkali and rare gas systems have demonstrated the importance of long-range dynamics in cold collisions. The result was that collision processes leading to trap loss, and taking place at relatively short

^a e-mail: fioretti@mail.df.unipi.it^b e-mail: arimondo@difi.unipi.it^c Laboratoire Aimé Cotton is associated with Université Paris-Sud.

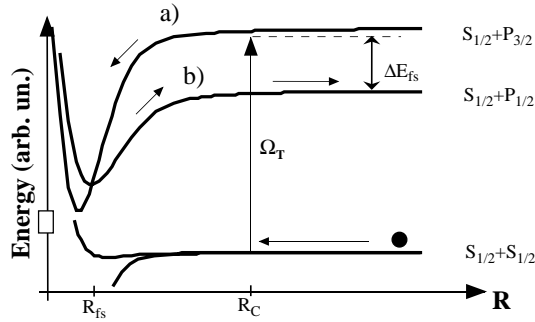


Fig. 1. Schematic representation of a FSC collision in cesium. The two excited-state molecular potentials are the 0_u^+ components of $b^3\Pi_u$ (a), and of $A^1\Sigma_u^+$ (b), respectively.

interatomic distance ($\sim 10\text{--}400a_0$, with a_0 the Bohr radius) can be either enhanced or suppressed by a previous excitation at long-range ($\sim 1500\text{--}3000a_0$). Enhancement [9–14] or suppression [8,9,12] originates because the colliding atom pairs are excited respectively to attractive or repulsive quasimolecular potentials. In their excited-state evolution, atom pairs are either pushed toward each other, or kept apart by the resonant dipole interaction, thus modifying the flux reaching short internuclear distances. When excitation is directed towards attractive potentials, processes involving atom pairs with relative angular momentum higher than that allowed by the low atomic velocity also contribute to the collision [14].

In this work, we model the cesium FSC trap losses within a picture that includes the flux enhancement. We demonstrate that the analysis of cold collisions in a cesium MOT should include the process of hyperfine optical pumping within a single collision, from the upper to the lower HF manifold in the ground state. This process, already considered by the Bagnato group for sodium photoassociation experiments without a precise modelling [15], stems naturally from the flux enhancement, and from the rich molecular hyperfine structure in the excited state.

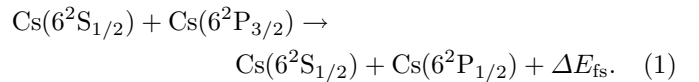
The present analysis is based on the complete knowledge of the excited-state HF manifold of the cesium dimer, whose computation is reported here. It allows us to restrict the possible dynamical schemes leading to the FSC process, and to point out the role played by the flux enhancement mechanism in our previous measurements of the FSC rate coefficient [4]. As a major difference with respect to the other cases of flux enhancement [8–14], here the same trap laser excites cesium atom pairs at long- and at shorter-range, starting from different hyperfine ground states. In respect to our previous analysis of reference [4], the present one aims to improve the physical interpretation of the FSC process in a MOT, in order to fit our data with a restricted number of parameters. In the previous analysis in fact, even if the final fitting function nicely reproduced the data, a relatively large set of fitting parameters was required. Moreover, several *ad-hoc* hypotheses on the laser excitation and on the excited-state survival were introduced. On the contrary, the available excited state HF manifold computation allows us to estimate the

branching ratios for HF state optical pumping during collisions.

In Section 2, the FSC and the flux enhancement processes are examined. In Section 3, the flux enhancement in FSC trap losses is described for cesium, even if our model can be applied to other trap loss processes as well. Section 4 reports the calculation of the molecular hyperfine structure of the $6P_{3/2}$ cesium excited state. Section 5 applies the model to the analysis of FSC losses, and Section 6 reports the conclusions.

2 Fine-structure changing process and long-range excitation

The excitation transfer with FSC in collisions between cesium atoms is described by the reaction



The first theoretical interpretation was given by Dashevskaya *et al.* [16], who individuated the molecular crossings, taking place at different interatomic distances R_{fs} , producing the reaction of equation (1). A renewed interest on the FSC process was associated to laser cooling and trapping of atoms in magneto-optical traps. In a MOT, cold atom pairs excited by the trapping laser to the $n^2P_{3/2}$ fine-structure branch and remaining in that state until they reach the R_{fs} distances, could produce FSC. As the ΔE_{fs} released as kinetic energy of the colliding pair is typically much larger than the trap depth, FSC collisions are an important process in MOT losses.

A detailed analysis of cold FSC collisions performed by Julienne and Vigué [17] showed that the leading contribution for cesium originates from the spin orbit mixing of the two attractive 0_u^+ components of the $A^1\Sigma_u^+(6^2P_{1/2})$ and $b^3\Pi_u(6^2P_{3/2})$ states (see Fig. 1), which have a short range crossing at $R_{fs} \sim 10a_0$ [16,17]. Among the five attractive Hund's case (c) electronic states connected to the upper $6^2P_{3/2}$ branch (0_u^+ , 1_g , 2_u , 0_g^- , and 1_u), the 0_u^+ state represents the only long-range incoming channel for this FSC mechanism. We note incidentally that a different picture arises for lighter alkalis, where Coriolis coupling becomes important. Predissociation of both the 0_u^+ and 1_g states of the ^{39}K to the lower fine-structure branch has been directly observed in reference [5] by resonance enhanced ionization of the $4P_{1/2}$ atoms.

When the hyperfine structure is included into the calculation of the cesium molecular potentials, it becomes apparent that the 0_u^+ state is adiabatically connected only to the lower part of the *lower* HF bundle of the excited-state manifold, as depicted in Figure 2b. On the other hand, in a standard cesium MOT almost all the ground state atoms are kept in the 4_g state by the repumping laser, and the excitation by the trap laser populates states right below the asymptotes of the *upper* HF bundle (Fig. 2a). Because the non-adiabatic coupling between these states and those connected to 0_u^+ is negligible (due to their large

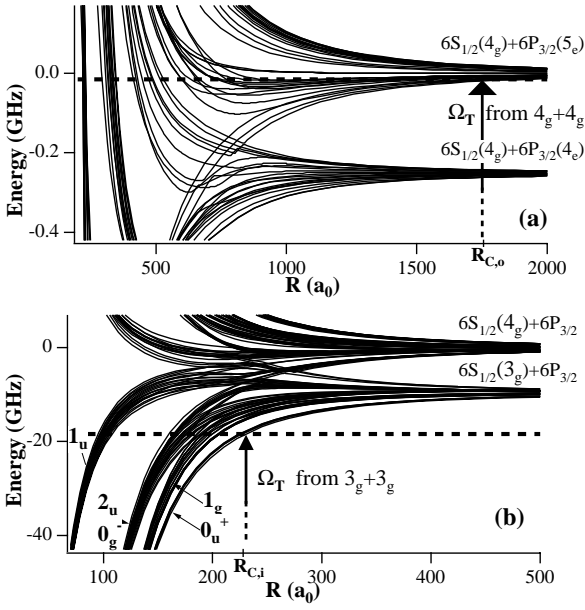


Fig. 2. Calculated long-range part of the Cs_2 adiabatic potential curves with hyperfine structure included (see Sect. 4 for details). In (a), attractive and repulsive states asymptotically connected to the uppermost $6^2S_{1/2}(4_g) + 6^2P_{3/2}(5_e)$ and $6^2S_{1/2}(4_g) + 6^2P_{3/2}(4_e)$ asymptotes. In (b), attractive states below the $6^2S_{1/2} + 6^2P_{3/2}$ branch. The dashed lines correspond to the energies of the molecular asymptotes, $4_g + 4_g$ and $3_g + 3_g$, respectively for (a) and (b), dressed with a trap laser photon. The zero of the energy scale is taken at the $4_g + 5_e$ asymptote.

energy distance and the absence of molecular crossings), no FSC collisions are expected to take place. Within this simple picture, the experimental results [4,6] cannot be easily explained. In fact, FSC collisions were observed also in a standard cesium MOT, containing atoms only in the upper hyperfine state. In rubidium, FSC collisions are also observed [7], although with a lower rate than in cesium, starting from the both HF asymptotes, so the picture in that case is not clear as well.

The flux enhancement in a cesium MOT proceeds through long-range excitation of one of the five attractive potential curves corresponding to 0_g^- , 1_g , 0_u^+ , 1_u , and 2_u states [18], which behave asymptotically as $-C_3/R^3$. Given the different asymptotic R -dependence of the ground-state potential, which is $-C_6/R^6$, and the relative magnitude of dispersion coefficients (in cesium $C_6 \sim 6500e^2a_0^5$ and $C_3 \sim 2-20e^2a_0^2$) in the long-range region $R \sim 1000-3000a_0$ the ground-state curves are essentially flat while the excited-state ones are already strongly attractive. A laser red-detuned from resonance by the quantity Δ excites atom pairs to an attractive quasimolecular state, preferentially at the Condon distance $R_C = (C_3/\hbar\Delta)^{1/3}$. In the excited state, the colliding pair is subject to the attractive resonant dipole force propelling the two atoms towards each other. The action of the force ends when spontaneous emission occurs, and the pair returns into the ground state. In this way, exoergic

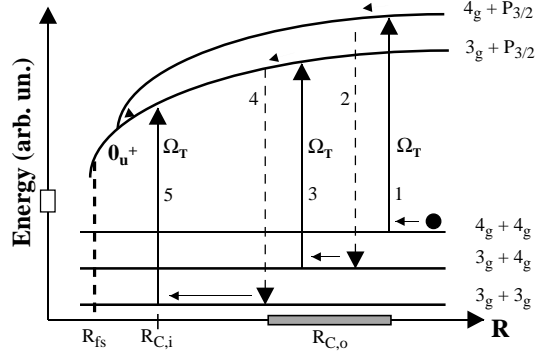


Fig. 3. Schematics of the optical pumping process between different ground state HF channels within a single collision, produced by the enhancement effect in a Cs MOT. Several hyperfine channels, from 5_e to 2_e are associated to the $^2P_{3/2}$ excited state.

binary processes which take place at shorter internuclear distance, can be enhanced [9–14]. *Vice versa*, in the case of a blue-detuned laser [8,9,12], repulsive potentials are excited and shielding occurs.

For intense trap lasers, the Condon distance R_C is power broadened to a region, generically indicated as $R_{C,o}$ in Figures 2a and 3. The atom pair can undergo several excitation/spontaneous emission cycles (*population recycling* [2]), and be accelerated during each time lap spent in the excited-state. This enhances the effects of the attractive force, and atomic pairs can get a relative velocity corresponding to a temperature of some mK [14], *i.e.* much higher than the cold atom temperature ($\sim 300 \mu\text{K}$ in our case).

3 The flux enhancement model

In cesium the atomic hyperfine structure produces different molecular asymptotes: 3 in the ground- and 2×4 in the $^2S_{1/2} + ^2P_{3/2}$ excited-state. The key idea of our model is that, given the long duration of a cold collision, the flux enhancement and the population recycling combine together during a single collision to produce optical pumping between different HF levels. The process is depicted in Figure 3. An atom pair, which starts approaching on the $4_g + 4_g$ channel, is excited by the trapping laser at $R_{C,o}$ to an attractive state connected to the $4_g + 5_e$. The pair returns to the ground-state by spontaneous decay either into the $4_g + 4_g$, or into the $3_g + 4_g$ continuum by emitting a blue-shifted photon. The latter process is forbidden by the atomic electric-dipole selection rules, but slightly permitted in the quasimolecular environment. In particular, the selection rule completely disappears, as it will be shown in Section 4, when the excited pair approaches regions where crossings from potential curves with different asymptotic hyperfine character occur. Once returned into the ground state, the colliding pair can be re-excited, still in the $R_{C,o}$ region, to quasimolecular attractive states below the $3_g + 5_e$ branch. There, the pair is further accelerated, and again can spontaneously decay partly

onto the lowermost $3_g + 3_g$ ground-state hyperfine asymptote.

These pairs are now available for the last shorter-range excitation by the trap laser (step 5 of Fig. 3) onto the 0_u^+ state. The Condon distance $R_{C,i} \sim 150\text{--}250a_0$ (Fig. 2b) of the last excitation is definitely shorter than the typical $R_{C,o}$ values because the trap laser is detuned by twice the 9.2 GHz ground-state HF separation. At $R_{C,i}$, the 0_u^+ potential curve is already strongly attractive, and excited pairs have the time to vibrate several times before radiatively decaying. During these molecular vibrations, the pairs can produce FSC loss, with probability P_{fs} .

We associate the occurrence of FSC collisions in our cesium MOT to the sequence of processes depicted in Figure 3. The use of a strong trap laser, well above the atomic saturation intensity, makes the flux enhancement and the population recycling the two leading phenomena. The process of optical pumping during the collision, greatly enhanced by the radiative recycling of a single colliding pair, can proceed through both short-living (with 0_u^+ , 0_g^- , and 1_g character) and long-living attractive states (with 1_u , and 2_u character). Former states, with a molecular radiative lifetime shorter than the atomic one [17], allow more cycles, but with low probability of optical pumping. Long-living states guarantee a longer excited-state survival, higher pumping probability, but fewer cycles. The important role of the long-living 1_u and 2_u states in producing flux enhancement has already been pointed out in references [11,19] in a rubidium MOT. Optical pumping is expected to be most efficient at internuclear distances where molecular potentials with different HF character cross each other, *i.e.* where the resonant dipole interaction is of the same order as either the ground- or excited-state hyperfine structure (see Fig. 2).

4 Molecular hyperfine structure

To support our hyperfine pumping scheme we have computed the cesium molecular potential curves for the first excited-state $6S+6P$, including fine and hyperfine structures. Potential curves covering all the explored internuclear distances have been obtained by correlating at $R \sim 20a_0$ the precise quantum chemistry calculation by Spiess [20] with the asymptotic calculation of reference [21]. Then, the fine-structure is included in these potentials by an R -dependent diagonalization of the various spin-orbit matrices. A more precise calculation of the asymptotic part of the curves has then been performed by diagonalizing the R -dependent interaction between the atom pair. The interaction includes of course the first terms of the multiple expansion: C_3/R^3 , C_6/R^6 , and C_8/R^8 , taken from reference [21], but also the fine and hyperfine interaction. The diagonalization is done in a two-atom basis in which fine and hyperfine interactions are diagonal [22]. The only good quantum numbers are the projections M on the molecular axis of the total angular momentum $F = F_g + F_e$, and the symmetry e of the wavefunction with respect to the atom exchange: $e = 1$ (-1) if the wavefunction is symmetrical (antisymmetrical).

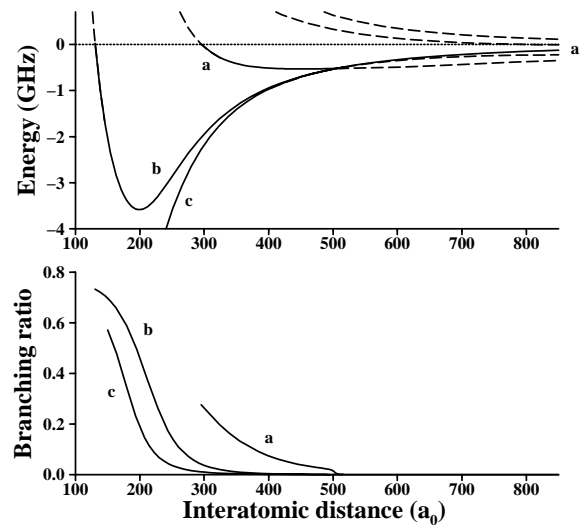


Fig. 4. Upper graph: molecular potential curves connected to the $4_g + P_{3/2}$ asymptotes, for the particular case of $M = 7$. Lower graph: branching ratio (defined as the ratio between the sum of the electronic matrix elements of the spontaneous emission towards $3_g + 3_g$ and $3_g + 4_g$, and the sum of the intensities towards $3_g + 3_g$, $3_g + 4_g$, and $4_g + 4_g$) corresponding to selected parts of the potential curves indicated by solid line in the upper graph. The selection is done by starting from the incoming channel $4_g + 5_e$ (curve a in the upper graph) and by following it either adiabatically (curve a) or diabatically through tiny avoided crossings (curves b and c). In addition, we have suppressed the $E > 0$ part of the curves, since they are not relevant for the present analysis.

Due to the large nuclear angular momentum of cesium ($I = 7/2$), a very large number of electronic states (1024), is obtained for the $6S_{1/2} + 6P_{3/2}$ asymptote, with M values ranging from 0 to 9 and $e = \pm 1$. The results were already shown in Figure 2, and the particular case of $M = 7$, $e = -1$ is shown in Figure 4a.

An extremely large number of avoided molecular crossings between curves of the same symmetry are possible, with various degrees of adiabaticity. We computed a number of them in the two regions where the resonant dipole interaction is of the same order of the atomic hyperfine separation in the ground and in the excited state, which correspond to $R \sim 150\text{--}250a_0$ (Fig. 2b), and $R \sim 400\text{--}800a_0$ (Fig. 2a) respectively. The size of these crossings vary from 1 MHz to several hundred MHz. By calculating the passage as a Landau-Zener process, we found all possibilities going from complete adiabaticity to complete diabaticity. As a consequence, during a cold collision, an atom pair, which is excited onto an attractive curve connected to the $4_g + 5_e$ asymptote, has non-zero probabilities to follow a lot of curves, either adiabatically or diabatically, through the numerous avoided crossings (see Fig. 4a). Due to the mixing between attractive and repulsive curves, the average value of F_e , and the probability to radiate towards states involving $F_g = 3$ may change a lot during this evolution.

Among all M and e values, we have selected the most probable potential curves and we have computed the

corresponding R -dependent electronic matrix elements for spontaneous decay towards the different ground-state hyperfine curves: $I(3_g + 3_g)$, $I(3_g + 4_g)$, and $I(4_g + 4_g)$, as well as the branching ratio towards $F = 3$, given by $(I(3_g + 3_g) + I(3_g + 4_g)) / (I(3_g + 3_g) + I(3_g + 4_g) + I(4_g + 4_g))$. The example of $M = 7$, $e = -1$ given in Figure 4b, although simple, is quite typical. The HF optical pumping, which is the basis of our model, is clearly allowed. In fact, colliding atom pairs at the crossing, either keep diabatically on the same attractive curve until spontaneous decay arrives, or adiabatically follow the repulsive one coming from the lower hyperfine, eventually being reflected and finally spontaneously decay. In the former case the wavefunction representing the colliding pair will maintain the same HF character till much shorter internuclear distances are reached. In the latter case instead, the wavefunction will change character, thus becoming a good candidate for an HF optical pumping process (see Fig. 4b). These results lead us to the conclusion that the general picture required by our model of hyperfine optical pumping within a single collision is plausible. We will now proceed with the implementation of our model, and with the fit of the experimental data.

5 Discussion of the results

In the experiment of reference [4], FSC trap losses were explored as a function of the operating parameters of the magneto-optical trap, without a catalysis laser. The photon yield on the D_1 line was recorded, and a simultaneous measurement of the density and of the total number of trapped atoms allowed the determination of the FSC rate coefficient β_{fs} . The β_{fs} data as a function of the measured hyperfine ground-state occupation $f_{F_g + F_e}$ and of the total intensity $I_T = I_{sat} \Omega_T^2 / \Gamma^2$ of the trap laser (where $I_{sat} = 2.21$ mW/cm²), are reported in Figure 5. The ground-state HF occupation was varied in two different ways: first, in a standard type I MOT, by reducing the intensity of the repumping laser, and second by changing the repumping scheme and realizing a mixed type I-II MOT [23].

Data for the type-I MOT are fitted (continuous lines in Fig. 5a) with the function

$$\beta_{fs} = \beta_0 (C_{4-4} + C_{3-4}) P_{fs} \quad (2)$$

with

$$C_{4-4} = (1 - f_{3_g + 4_e})^2 P_{2-exc} P_{HFC}^2 P_{C,i} \quad (3)$$

$$C_{3-4} = f_{3_g + 4_e} (1 - f_{3_g + 4_e}) P_{1-exc} P_{HFC} P_{C,i} \quad (4)$$

where $\beta_0 = 4\pi R_{C,o}^2 v_{C,o}$ represents the maximum rate coefficient occurring if all pairs excited at long-range were to produce trap-loss (for unitary excitation probability), P_{HFC} is the branching ratio for decay into the lower hyperfine manifold, and P_{fs} final probability for the FSC process.

The terms C_{4-4} and C_{3-4} describe the dynamic evolution, from $R_{C,o}$ to $R_{C,i}$, of pairs colliding along the $4_g + 4_g$

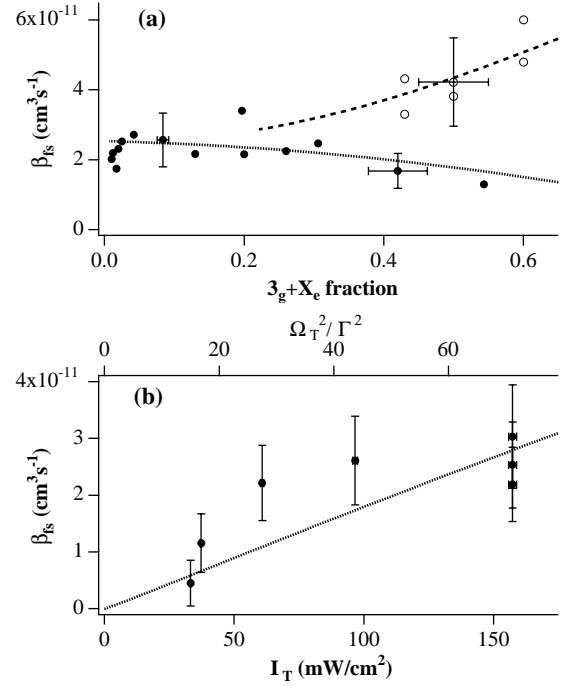


Fig. 5. In (a) β_{fs} data and fit as a function of $f_{3_g + X_e}$ with $X = 2-4$, the hyperfine state occupation. Filled (\bullet), and empty (\circ) circles are data for the type-I, and mixed type-I type-II MOT's respectively [4], obtained by varying the repumping laser intensity. In (b) β_{fs} data and fit as a function of intensity of the trap laser, for the type-I MOT. Fitting parameters are in the text.

and $3_g + 4_g$ channels. P_{n-exc} is the probability for n excitations in the $R_{C,o}$ region, and is calculated, as a function of the trap laser intensity, as a series of n Landau-Zener processes [10] occurring at different internuclear distances, after $n-1$ spontaneous emissions. Each spontaneous emission is considered to take place with a delay of the order of the molecular lifetime after the excitation. Each reexcitation is considered to take place after a motion in the ground state, which duration is a function of laser intensity. $P_{C,i}$ is the excitation probability at $R_{C,i}$, also calculated as a Landau-Zener process.

The fit of data for the mixed type I-II trap [4] (dashed line of Fig. 5a) is obtained by adding a term to equation (2), thus giving

$$\beta_{fs} = \beta_0 (C_{4-4} + C_{3-4} + \epsilon C_{3-3}) P_{fs} \quad (5)$$

where

$$C_{3-3} = f_{3_g + 2_e}^2 P_{C,i}. \quad (6)$$

The new term represents the contribution of the $3_g + 3_g$ incoming channel, which is fed at long-range by the intense repumping laser tuned below the $3_g \rightarrow 2_e$ atomic transition. This term does not require a hyperfine pumping probability. ϵ is a fit parameter quantifying the relative contribution of the new channel.

For all the calculations, we used the parameters (lifetime, dipole moment) of the 0_u^+ molecular state. For the short term FSC probability, we use the value $P_{fs} = 0.84$, resulting from the sum over all molecular vibrations [24], of the nonadiabatic FSC probability $\eta_{fs} = 0.28$ calculated in reference [17]. Fitting simultaneously the three data sets of Figure 5, for a value of the initial cesium velocity $v_{C,o} = 20$ cm/s, we have obtained $R_{C,o} = 1260a_0$, $P_{HFC} = 0.67$, and $\epsilon = 1.6$. The fitted value for $R_{C,o}$, which acts as an overall scale factor, is close to the expected one, and make us confident of the reliability of the model. The value of P_{HFC} derived from the fit is large compared to that derived from the molecular potentials of Figure 4b, for the large internuclear distance R where the decays from the 0_g^- state are supposed to occur. We associate this result to one of the limitations of the present model, which considers only 2 and 1 excitation processes, for the $4_g + 4_g$ and the $3_g + 4_g$ incoming channels respectively, as discussed in the following paragraphs. A more elaborated model, including a larger number of reexcitation processes, would produce a decrease of P_{HFC} . Finally the relatively large value of ϵ for fitting the mixed type I-II MOT data, indicates the important role of pairs excited onto the $3_g + 2_e$ manifold, surviving till they reach the inner range where FSC occurs.

We have verified that in the type-I MOT data, the inclusion of a term C_{3-3} proportional to $f_{3_g+4_e}^2$ does not improve the fit quality. This demonstrates that the main contribution to FSC process arises from pairs that have undergone excitation at long-range, and optical pumping. From the fit versus the trapping laser intensity we derive a slope for β_{fs} of 1.8×10^{-13} cm⁵ s⁻¹ mW⁻¹. A comparison between this value and the total trap-losses reported in references [25, 26] shows that FSC losses is between one third and one sixth of the total losses. This is in reasonable agreement with the recent accurate measurements of Shaffer *et al.* [6], where FSC loss result one half of the total losses, in the same range of trapping laser intensities.

The presented model is primarily intended to provide a phenomenological but physically significant framework to explain and fit the FSC collisional process between cold cesium atoms. In this respect we believe we produced a clear picture. Nevertheless, a number of points needs to be discussed in order to state the limitations of the model, and of its predictive capabilities. First, the excitation has been always considered to be directed to a single molecular vibrational level. This would be the case if the vibrational spacing were much larger than the convolution between the laser and the level linewidths. While this approximation is partially justified for the shorter-range excitation (step 5 of Fig. 3), this is surely not true for in the case of the long-range ones (steps 1 and 3 of Fig. 3), given the number of levels generated by the rotational and hyperfine interactions. Excitation to a distribution of bound states, belonging to all the different electronic states, would be much closer to reality, but its implications (coherent excitation, wave-packet dynamics, coupled multichannel analysis) are obviously beyond the scope of this paper. We stress that such a level of accuracy in the modelling, al-

though not required for explaining our FSC data, could be required by the continuously improving status of the art in cold collisions experiments [6, 7, 11–14]. A detailed comparison among the different theoretical approaches actually available in cold collisions can be found in reference [27].

A second but related point is the use of the parameters of the 0_u^+ state for the final fit. Its use in the shorter-range excitation (step 5 of Fig. 3) is justified, while for the long-range one an weighted average among the possible excitations of the different electronic states could be considered. As the final fit results are expected to change, this is also a limitation of our the present analysis. Nevertheless a result that can be extracted by our fit is that, in the explored high intensity regime $\Omega_T/T \gg 1$ of our MOT, the optical pumping during the collision is very likely to happen for roughly half of the initial colliding pairs. This means that the “memory” of the initial hyperfine states in such a collision is very low.

Finally, our model fails to predict the saturation of β_{fs} with the trap laser intensity, which shows up in the data of Figure 5b and is confirmed by recent data of reference [6]. This is because the last excitation at $R_{C,i}$ is not saturated, at the explored trap laser intensities. Moreover, reference [28] reports saturation of the rate coefficient as a quite general feature of different trap loss processes taking place in magneto-optical traps. This behavior is described introducing a non radiative decay process, which is explained in terms of coupling between optically active and optically inactive molecular states [28], which should be included in the present model. A complete theoretical analysis similar to that in presented in reference [27] would be required for deriving the saturation.

For what concerns the temperature dependence of the FSC process, we notice that it can be easily included in our fit by using a temperature-dependent outer velocity $v_{C,o}(T)$. We have verified that the present fit does not change significantly if such dependence is introduced.

All the present calculation of the excited-state potentials, and relative discussion about the adiabaticity of the crossing has been done for s -wave collisions. On the contrary, it has been observed that more partial waves, up to $l \sim 6$ contribute to cold collisions in a cesium MOT [14]. The inclusion of the centrifugal term $\hbar^2 l(l+1)/2mR^2$ changes the potential curves, and thus the characteristic of the crossings that have been discussed so far. Nevertheless the magnitude of the changes remain small in the considered range of interatomic distances (≤ 1 MHz for $R \sim 500a_0$), and the main points of the discussion should not be affected.

6 Conclusion

In conclusion, from the analysis of cesium ground-state and excited-state long-range potential curves calculated including the hyperfine structure, we derived a dynamical evolution providing a possible explanation of the occurrence of FSC collisions in a cesium MOT. This scheme,

which differs from the widely used semiclassical Gallagher-Pritchard model [24, 17] for cold collisions, is strongly dependent on the flux enhancement provoked by the long-range excitation by the trap laser, leading to HF optical pumping within a single collision. This model is used to fit cesium FSC loss data with a restricted number of parameters.

The description of cold collisions in presence of a laser field is very different depending if the laser field is either almost resonant or detuned with respect to the atomic resonance. This correspond to the two cases in which the excited (quasi)molecule either does not or does have the time to complete a single vibration before radiative decay. We showed that both situations can be present in a MOT even in presence of the trapping and repumping lasers alone.

Within the present model some features of our data are still not reproduced (*i.e.* saturation at large laser intensity), and the influence of other experimental parameters has not been discussed (*i.e.* the role of the repumping laser). In this respect, a different and more complete approach would be necessary, in order to realistically describe the multichannel long-range excitation and dynamics. Nevertheless, this HF optical pumping effect, which is peculiar of cold collisions, does play a role in producing FSC in cesium MOT, and probably also in other alkali magneto-optical traps, so it needs to be included in a correct description of cold collisions.

The flux enhancement and the hyperfine optical pumping mechanisms can provide short-range excitation at $R_{C,i}$ to attractive electronic states other than the 0_u^+ . In particular, excitation of the 0_g^- state, which has demonstrated to provide an efficient decay rate into ground-state cold Cs_2 molecules [29], is possible. As shown in reference [29], a photoassociation laser detuned 18 GHz from resonance is very efficient in producing 0_g^- excited molecules, which subsequently decay also into $a^3\Sigma_u^+$ translationally cold, ground state molecules, which are observed. As cold molecules are observed in cesium also under absence of a specific photoassociation laser, two different formation mechanisms were proposed: three-body recombination [30] and photoassociation produced directly by the trapping and the repumping lasers [29]. The model presented here can provide a possible dynamical scheme which can explain the production of Cs_2 molecules in a MOT even in absence of a specific photoassociation laser. As the two mechanisms yield a different dependence on the experimental parameters (atomic density, laser intensity), specific experiments are needed to clarify their respective role.

Stimulating discussions with Paul Julienne, Maria Allegrini, N.P. Bigelow, Jörg H. Müller, Olivier Dulieu, Françoise Masnou-Seeuws, and Pierre Pillet are gratefully acknowledged. This present research was supported by the European Community through TMR Network Grants No. FMRXCT96002 and FMBICT961218, by the Consiglio Nazionale delle Ricerche of Italy through a Progetto Integrato and by the PRA on Bose-Einstein Condensation of the INFN-Italy.

References

1. T. Walker, P. Feng, *Adv. At. Mol. Opt. Phys.* **34**, 125 (1994).
2. K.-A. Suominen, *J. Phys. B: At. Mol. Opt. Phys.* **29**, 5981 (1996).
3. J. Weiner, V.S. Bagnato, S.C. Zilio, P.S. Julienne, *Rev. Mod. Phys.* **71**, 1 (1999).
4. A. Fioretti, J.H. Müller, P. Verkerk, M. Allegrini, E. Arimondo, P.S. Julienne, *Phys. Rev. A* **55**, R3999 (1997).
5. H. Wang, P.L. Gould, W.C. Stwalley, *Phys. Rev. Lett.* **80**, 476 (1998).
6. J. Shaffer, W. Chalupczak, N.P. Bigelow, *Eur. Phys. J. D* **7**, 323 (1999).
7. L.G. Marcassa, R.A.S. Zanon, S. Dutta, J. Weiner, O. Dulieu, V.S. Bagnato, *Eur. Phys. J. D* **7**, 317 (1999).
8. L. Marcassa, R. Horowicz, S. Zilio, V. Bagnato, J. Weiner, *Phys. Rev. A* **52**, R913 (1995).
9. M. Walhout, U. Sterr, C. Orzel, M. Hogerland, S.L. Rolston, *Phys. Rev. Lett.* **74**, 506 (1995).
10. V. Sanchez-Villicana, S.D. Gensemer, P.L. Gould, *Phys. Rev. A* **54**, R3730 (1996).
11. S.D. Gensemer, P.L. Gould, *Phys. Rev. Lett.* **80**, 936 (1998).
12. C. Orzel, S.D. Bergeson, S. Kulin, S.L. Rolston, *Phys. Rev. Lett.* **80**, 5093 (1998).
13. H.C. Mastwijk, J.W. Thomsen, P. van der Straten, A. Niehaus, *Phys. Rev. Lett.* **80**, 5516 (1998).
14. A. Fioretti, D. Comparat, C. Drag, T.F. Gallagher, P. Pillet, *Phys. Rev. Lett.* **82**, 1839 (1999).
15. L.G. Marcassa, G.D. Telles, S.R. Muniz, *Phys. Rev. A* **60**, 1305 (1999) and references therein.
16. E.I. Dashevskaya, A.I. Voronin, E.E. Nikitin, *Can. J. Phys.* **47**, 1237 (1969).
17. P.S. Julienne, J. Vigué, *Phys. Rev. A* **44**, 4464 (1991).
18. Excitation of the 2_u state from the ground state, although electric dipole forbidden, is permitted at long-range through retardation effects.
19. P.D. Lett, K. Molmer, S.D. Gensemer, K.Y.N. Tan, A. Kumarakrishnan, C.D. Wallace, P.L. Gould, *J. Phys. B: At. Mol. Opt. Phys.* **28**, 65 (1995).
20. N. Spiess, Ph.D. thesis, Fachbereich Chemie, Universität Kaiserslautern, 1989, unpublished.
21. M. Marinescu, A. Dalgarno, *Phys. Rev. A* **52**, 311 (1995).
22. D. Comparat, C. Drag, A. Fioretti, B. Laburthe Tolra, A. Crubellier, O. Dulieu, F. Masnou-Seeuws, P. Pillet, *Eur. Phys. J. D* **11**, 59 (2000).
23. E.L. Raab, M. Prentiss, A. Cable, S. Chu, D.E. Pritchard, *Phys. Rev. Lett.* **59**, 2631 (1987).
24. A. Gallagher, D. Pritchard, *Phys. Rev. Lett.* **63**, 957 (1989).
25. D. Sesko, T. Walker, C. Monroe, A. Gallagher, C. Wieman, *Phys. Rev. Lett.* **63**, 961 (1989).
26. C.G. Townsend, D. Phil. thesis, Oxford University, UK 1995, unpublished.
27. K.-A. Suominen, Y.B. Band, I. Tuvi, K. Burnett, P.S. Julienne, *Phys. Rev. A* **57**, 3724 (1998).
28. J.P. Shaffer, W. Chalupczak, N.P. Bigelow, *Phys. Rev. A* **61**, 011404 (2000).
29. A. Fioretti, D. Comparat, A. Crubellier, O. Dulieu, F. Masnou-Seeuws, P. Pillet, *Phys. Rev. Lett.* **80**, 4402 (1998).
30. T. Takehoshi, B.M. Patterson, R.J. Knize, *Phys. Rev. A* **59**, R5 (1999).